University of Copenhagen

Niels Bohr Institute

Permeability studies of protein effects on the nearby membrane by Monte Carlo simulations

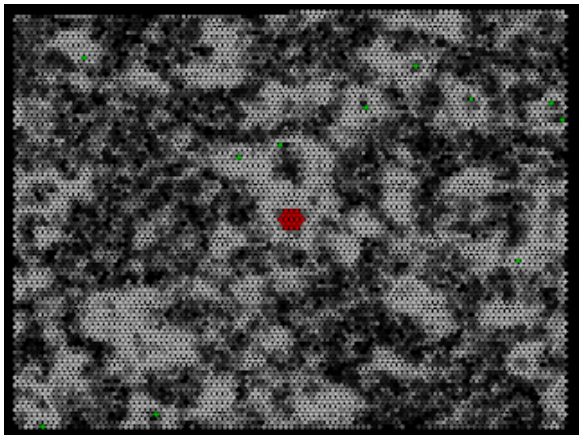

A BACHELOR PROJECT

Lars D. Mosgaard

Vedran Sekara

Submitted May 29, 2009

Preface

Front page picture shows a fluctuation snapshot of the simulated membrane. The snapshot is taken at phase transition temperature. Red dots illustrate a protein, green dots illustrate pores. The fluctuations are are illustrated by a greyscale where white means maximal fluctuations.

Resumé

Vi har i dette projekt undersøgt om proteiner kan pårvirke den omkringliggende lipidmembran sådan, at den udviser egenskaber (channel events) der ellers typisk kun er tilskrevet proteinerne selv. Dette er blevet gjort ved brug af en simpel model for en biologisk membran. Vores model er baseret på en 1,2-dipalmitoy- lphosphatidylcholine (DPPC) lipidmembran hvori et enkelt simpelt protein er indlejret.

Med denne model har vi undersøgt hvordan proteinets interaktioner med lipiderne påvirker permeabiliteten. Yderligere har vi studeret, hvordan ændringerne i membranens interne interaktioner påvirker proteinets effekt.

Vi har fundet klare indikationer på, at proteiner inducerer store lokale ændringer i membranens egenskaber, heriblandt permeabiliten. Disse inducerede ændringer kan variere fundamentalt ved ændringerner af proteinets interaktioner med membranens lipider. Både permeabilitets-fremmende og -hæmmende proteinadfærd er blevet observeret i en omfattende grad. Vi fandt yderligere, at små ændringer af membranens interne interaktioner påvirker proteiners effekt kraftigt. Alt dette udmunder i krafig indikation af at channel events kan tilskrives membranen.

Resultaterne i dette projekt er blevet simuleret ved hjælp af Monte Carlo metoden. Vi har i simuleringerne benyttet to-tilstands Ising modellen til at beskrive lipidmembranens adfærd. Parametrene til Monte Carlo metoden er fundet gennem Differential Scanning Calorimetry (DSC).

Acknowledgements

First we want to thank our supervisor Thomas Heimburg. He has been a great source of inspiration, and has been a great help in exploring the possibilities of our project.

Second we thank Andreas Blicher. In almost all research one stands on the shoulders of titans. The titan just under us is Andreas. He has supplied us with most of the program used in this project, and has been patient explaining the details of the program to us. He has further helped us with the experimental part of the project, and always been willing to help.

We last want to thank all of The Membrane Group for letting us be a part of the team, especially Julia, who was always been available with a helping hand.

Contents

Part I
Introduction

Biological membranes define boundaries in biology. They surround living cells as well as many of their inner components and are essential for a broad spectra of vital processes. Understanding the physics of these structures can contribute to the understanding of the living cell.

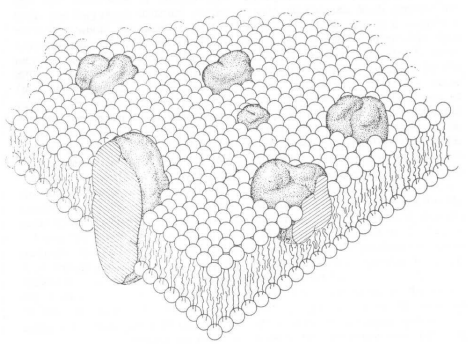

Figure 1: Illustration of an idealized patch of biological membrane. Small objects with tails are lipids, while larger objects are proteins. The figure is taken from [1].

Biological membranes are complex bilayer structures that are mainly composed of a large numbers of different types lipids and proteins.

Lipids (fig. 2) are amphiphilic molecules which consist of a hydrophilic head group and a hydrophobic tail. When in a water environment, lipids tend to aggregate shielding the hydrophobic tail from water. Aggregation leads to the formation of micelles or bilayer structures, hence planar bilayers or vesicles (see fig. 2). In general other non-lamellar phases exist, but they are hardly observed in excess water.

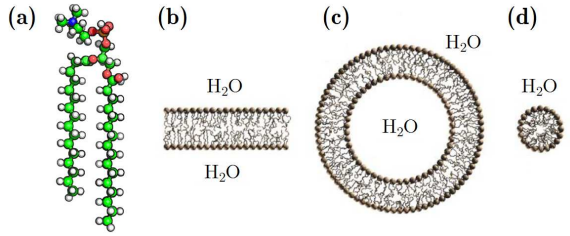

Figure 2: **A:** Illustration of a 1,2-dipalmitoylphosphatidylcholine (DPPC) lipid. **B:** A patch of a bilayer. **C:** Unilamellar vesicle **D:** Micelle. Illustrations are taken from [2].

Proteins are organic compounds made of amino acids arranged in linear chains, connected by peptide bonds. There are 22 standard amino acids and

each has rather unique properties e.g. charge. The variety in amino acid properties and the number of possible combinations, make proteins complex and versatile structures. Protein are regarded as absolutely essential in biological processes. In the context of membranes, proteins can either be adsorbed to the surface or be embedded (see fig. 1) [3].

Biological membranes function as selectively permeable barriers, where the lipid parts of the membrane often are regarded as permeable only for small molecules, e.g. water. Transportation of larger molecules and ions happens through channel protein. These protein create channels through the membrane where they may control the essential transportation.

Direct electrophysiological studies of protein activity, without including the effect of the nearby membrane, are impossible [4]. Though have electrophysiological events been attributed protein activity.

It has been shown that pure lipid membranes, near phase transition, display channel events similar to those attributed to channel proteins[4][5][6], and that these events are reversible [7][8][9].

These findings have led to the understanding, that *any* mechanism that leads to large fluctuations in a membrane will similarly induce channel events.

Studies have shown that proteins can induce large fluctuations in the neighboring membrane [4] and that protein induced changes affect a large number of lipids [10].

From this is not unreasonable to ask the question: Could it be possible that channel events typically attributed to proteins could originate from lipids, because the proteins influence the transition behavior in their environment?

1 Motivation

Interactions between proteins and lipids are essential in understanding all membrane processes, but are poorly understood on a microscopic level. A variety of simple models have been used to study these interactions with great success. Among these, are studies of variation in thickness of the lipids impact on embedded proteins. These studies have though mainly focused on changes in the protein configuration and their anchoring induced by lipids and not on the change in lipid configuration [11].

For this reason, the focus of this project will be to investigate protein influence on permeability of its neighboring lipid environment.

For a biological membrane model we have chosen 1,2-dipalmitoylphosphatidylcholine (DPPC) as lipid because of its well documented behavior and pronounced main melting phase transition. As model of a protein we have chosen to embed a single stable object that has well defined interactions with the lipids. With this simple model we aim to get theoretical indication

on whether the raised question can be true or not.

This is relevant because it can change the general understanding of membranes

To investigate the implications of our simple model we use the Monte Carlo method. The Monte Carlo method has been chosen over the mean-field theory due to its strength in simulating transition phenomena and the fact that it takes fluctuations of the environment into account. A further strength of the Monte Carlo method compared to more detailed methods, such as molecular dynamical simulations, is that it can describe the behavior of a large system within a realistic time frame. The used model in the Monte Carlo method is based on the two-state Ising model [12].

The main parameters used in the model are experimentally determined by differential scanning calorimetry (DSC).

Part II
Theory

This part will introduce the necessary theory for this project. It will include an introduction to membrane properties, the Monte Carlo method and the membrane model we used.

2 Membrane Properties

The phase transition is essential for biological membranes behavior.

2.1 Phase transition

For single lipid systems, phase transitions are defined as points where membranes change between two states. Phase transitions for lipids occurs at well defined temperatures. These transition temperatures depend on lipid composition (e.g. length of chains, double bonds between carbon-carbon atoms, head group size, etc.). The transition can be shifted by changing external values (e.g. pressure, pH value, etc.) or by adding additional molecules, such as proteins or anaesthetics. Most natural lipids have melting temperatures in the temperature regime $-20°$C to $60°$C.
The membrane melting temperature, T_m, is defined as the temperature where the lipids have an equal probability to be in one of two states. By calculating the difference in entropy, ΔH, and enthalpy, ΔS, between the two states (see appendix A), one can find the transition temperature to be:

$$\Delta H - T_m \Delta S = 0 \Leftrightarrow T_m = \frac{\Delta H}{\Delta S} \tag{1}$$

Membranes are bilayer structures which can exist in four different states depending on the temperature (listed in order of increasing temperature) [13]:

- L_c **state:** Crystalline state, in which the lipids are ordered in three dimensions.
- L'_β **state:** Crystalline molecular order. Chains are mostly 'all-trans' [1] ordered and tilted. This phase is often called the solid phase or simply the gel phase.
- P'_β **state:** So called 'ripple' phase. The membrane is partially solid, partially fluid and has a periodic structure. This phase forms prior to chain melting [14].

[1] Spatial orientation of the two chains.

- L_α **state:** Lipid chains are disordered. Order of lattice is lost. This phase is often called the liquid-disordered phase or simply the fluid phase.

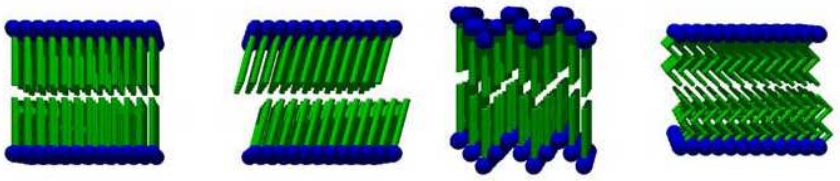

Figure 3: Illustration of different membrane states. **Left:** L_c state. **Middle left:** L'_β state. **Middle right:** $P_\beta state$. **Right:** L_α state. Taken from [15].

In this project we will ignore the transition between the gel and ripple phase and only consider lipids being in either gel or fluid phase. This can be justified by the choice of lipid membrane (DPPC), which only has a minor pre-transition away from the main transition. The transition between gel and fluid is illustrated in fig. 4.

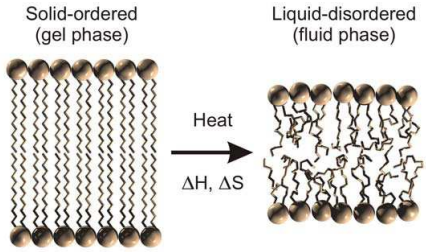

Figure 4: Illustration of a chain melting transition. Taken from [2].

2.2 Thermodynamic properties

Many thermodynamic properties can be derived from fluctuations of a system; among these is the heat capacity.

At constant pressure, the heat capacity, c_p, is defined as the difference in heat, dQ per difference in temperature, dT.

$$c_p = \left(\frac{\mathrm{d}Q}{\mathrm{d}T}\right)_p \tag{2}$$

Enthalpy is defined as $H \equiv U + pV$. The differential is $\mathrm{d}H = \mathrm{d}U + p\mathrm{d}V + V\mathrm{d}p$. By substituting d$U$, d$H$ will be reduced to $\mathrm{d}H = \mathrm{d}Q$, at constant pressure.

$$c_p = \left(\frac{\mathrm{d}H}{\mathrm{d}T}\right)_p \tag{3}$$

Which states that the heat capacity is directly related to the change in enthalpy[2].

The heat capacity at constant pressure can be derived from fluctuations using the fluctuation-dissipation theorem [16] (see appendix B).

$$c_p = \left(\frac{\mathrm{d}\langle H\rangle}{\mathrm{d}T}\right)_p \tag{4}$$

$$= \frac{\langle H^2\rangle - \langle H\rangle^2}{RT^2} \tag{5}$$

Where R is the gas constant. The heat capacity is obtained in the model through fluctuations in enthalpy using equation (5).

The fluctuations of the lipid membrane system are further correlated to the isothermal area compressibility. The compressibility is a measure of the relative area change of the system as response to a change in lateral pressure.

$$\kappa_T^A = -\left(\frac{1}{\langle A\rangle}\cdot\frac{\mathrm{d}\langle A\rangle}{\mathrm{d}\Pi}\right)_T \tag{6}$$

$$= \frac{\langle A^2\rangle - \langle A\rangle^2}{\langle A\rangle RT} \tag{7}$$

Where Π is the lateral pressure and the enthalpy in this case is $H = U + pV + \Pi A$.

2.3 Model for permeability

Lipid membranes are usually considered as insulators, which implies that the permeability of larger molecules and ions is often neglected. But in reality, due to diffusion, there is a finite probability for larger molecules to cross the membrane [14]. Studies have shown that the permeability of lipid membranes close to lipid melting transition is significantly increased [2][5].

The documented enhancement of the permeability has given rise to speculations on the nature of this phenomena. It has been stated that this can not alone be explained by passive diffusion of molecules through the hydrophobic parts of the membrane [14]. An likely explanation is the formation of pores in the membrane.

A formation of a pore will require a compression of the bilayer. The work needed to compress the bilayer is proportional to the lateral compressibility of the membrane. Since the compressibility of the membrane is directly proportional to the heat capacity [2], this will make the probability of forming a

[2]Same procedure can be done for the entropy, since $\mathrm{d}Q = T\mathrm{d}S$, so $c_p = T\left(\frac{\mathrm{d}S}{\mathrm{d}T}\right)_p$.

pore close to the transition high, which can explain the heighten permeability. Further, the compressibility is high at domain interfaces e.g. fluid-gel or lipid-protein, which will make the appearance of pores more likely in these areas.

2.4 Hydrophobic matching

Different lipids have different chain length, even the same type of lipid has different chain length, depending on its state. By changing the state from gel to fluid a DPPC lipid changes it is chain length by $\sim 13\%$ [17]. A membrane, depending on the temperature of the system, will have different hydrophobic thickness.

Proteins as well as lipids, are composed of hydrophobic and hydrophilic parts. Since contact between hydrophobic parts and water is unfavorable, proteins can fold themselves such that they protect their own hydrophobic parts or embed themselves in lipid bilayers.

Figure 5: Illustration of two proteins embedded in a lipid membrane. Due to hydrophobic matching, the thickness of the membrane varies around the proteins. Taken from [2].

The thickness of the hydrophobic part of a protein embedded in a lipid membrane often differs from that of the bilayer. Leading to a hydrophobic mismatch where hydrophobic parts are exposed to water. The mismatch between lipid and protein will be minimized in the following ways [18]:

- Protein may aggregate, such that they shield their own hydrophobic regions by reducing the interface region with lipids. Thus, only the interface region will have a free energy contribution.
- The lipid membrane surrounding the protein can switch its state (either melt or freeze) such that the lipids form a shielding annulus. There is a free energy cost to change lipid state.
- If the membrane consists of different types of lipids, the protein can recruit lipids of similar hydrophobic length around itself [19].
- Change of conformation. By changing its structure a protein can change its hydrophobic length. A change in protein structure is connected to a change in function.

3 Monte Carlo method

The Monte Carlo method is a universal method that can be applied to a large range of systems. It is especially potent in the study of systems containing a large number of coupled degrees of freedom, e.g. gasses, liquids, polymers, and economics[3]. The number of possible states in these type of systems is astronomical.

For a system containing N particles, which can be in one of two states, the total number of states will be 2^N. For a small system containing $N = 100$, the number of states will be $2^{100} \simeq 10^{30}$, this being more than a supercomputer can compute in a lifetime. In the scope of this project we will need a system containing $1000 - 10000$ particles, and furthermore a lipid can in reality be in a vast number of states. From this it is obvious that direct evaluation is not possible.

The basic idea of the Monte Carlo method is to define a system and the dynamics that govern it. This gives a set of possible states. The Monte Carlo method chooses a random state μ and generates a new state ν of the system, in a random fashion[4]. The probability of generating the state ν given μ is called the transition probability $P(\mu \to \nu)$. The transition probability must not vary over time, and the transition probability must only depend on the properties of μ and ν, and not on any state the system previously has passed through. This ensures that the probability of generating ν given μ is conserved. The system is reaches equilibrium when the number of changes from state μ to state ν is equal to the number changes from ν to μ.

This simulated random walk through the states reaches, when equilibrated, a Boltzmann distribution around the most likely state, equal to that of the real system. The method can, after equilibrium is reached, estimate observable quantities (e.g. enthalpy, internal energy, entropy and heat capacity) of the real system.

As noted, the number of states in the systems of interest is astronomical. A random search for the subset of states that pose the Boltzmann distribution of the real system, will result in that equilibrium is never reached on a realistic time scale. The search for the wanted subset is in a Monte Carlo method is governed by a rejection algorithm, in our case the Glauber algorithm [20]. This algorithm ensures that a good estimate of the wanted subset of states is reached after a relatively short time.

[3]Monte Carlo simulations have no direct time scale included, but only simulate the equilibrium properties of the given system.

[4]Meaning that it will not necessary generate ν every time given μ.

3.1 Glauber Algorithm

The essence of the algorithm [20] is that given the choice between two states, the most likely should have a higher chance to be generated. This is in practice carried out in the following manner:

- A given start configuration of the system is stored and its Gibbs free energy is calculated.
- Let the system undergo minor changes, hereby changing the state of the system, and calculate the Gibbs free energy of this new configuration.
- The changes of the system are accepted with the probability

$$P = \frac{\exp\left(-\Delta G/RT\right)}{1+\exp\left(-\Delta G/RT\right)} \equiv \frac{K}{1+K} \tag{8}$$

  where ΔG is the difference in the Gibbs free energy between the two states and K is the Boltzmann factor.

From this the equilibrium between two configurations A and B is determined by

$$\frac{P_B}{P_A} = \exp\left(-\Delta G/RT\right) \tag{9}$$

this being the Boltzmann distribution, as required.

The weighting of states in the Glauber algorithm ensures that mainly the most relevant states are reached in finite iterations (Monte Carlo cycles). This enables the Monte Carlo method to make good estimates of the Boltzmann distribution of states within a relative small number of cycles. In general all states can be reached if the system is allowed to fully equilibrated. This ensures, by the ergodic theorem [14], that averaging one system for a long period of time[5] is equal to averaging over a large number of independent systems. This makes the Monte Carlo method a powerful tool since a single simulation can ensure a minimal statistical error on the average values.

[5] In the context of the method a long period of time is equal to a large number of Monte Carlo cycles

3.2 Model

To model a lipid membrane it is necessary to decide on a level of description. A membrane can be described on the atomic level, as well as on a coarse grained level where each lipid can only be in one of two states. The limitations on the number of states that can be simulated means that detailed simulation can only be done on very small systems, where it is possible to study large systems with more simple models. In this project we only consider behavior on a scale larger than a single lipid.

In our simulation we have used a model of a lipid membrane system, which is based on the Ising model [12]. The Ising model is essentially a two state model taking only nearest neighbor interactions into account. Originally made for describing transition in ferromagnets. The Ising model compared to more detailed models, such as the 10-state Pink model [21], is $100 - 1000$ times faster and the choice of model has no significant effect on the overall physical behavior of the system [22]. Furthermore the Ising model contains only a few parameters, which can be determined through calorimetric experiments [23].

The Ising Hamiltonian in the original form is given by

$$\mathcal{H} = -\frac{\epsilon}{2}\sum_{\langle i,j\rangle}\sigma_i\sigma_j - h\sum_i \sigma_i \tag{10}$$

where σ_i is the state, usually denoted by $\pm$, of a given site in the system. The first sum is over nearest neighbors, indicated by $\langle i, j\rangle$, and ϵ is the nearest neighbors interaction parameter. The last sum takes into account the influence of a external field, where h denotes the external field.

To describe the melting of a lipid membrane with the Ising model the following assumptions are needed [24][25]:

- Each lipid can only be in one of the two following states:
  - A gel state, with low enthalpy H_g and low entropy S_g
  - A fluid state, with high enthalpy H_f and high entropy S_f
- The lipids only interact with nearest neighbors. This is justifiable since the majority of interaction between lipids is due to Van der Waals interactions which have a distance dependence of $\frac{1}{R^5}$.
- All lipids, independent of state, are hexagonally packed on a two dimensional lattice, meaning that each lipid molecule has $z = 6$ nearest neighbors. Experiments have shown that lipid membranes in the gel state mainly have this packing [13], and for simplicity we assume that the lipids in the fluid state are similarly packed. This assumption has been discussed in the literature [24].

These assumption lead to the following Gibbs free energy [14][6]

$$G = G_g + N_f \left(\Delta H - T\Delta S\right) + N_{fg}\omega_{fg} \tag{11}$$

Essentially, G_g denotes the Gibbs free energy of the system when all lipids are in the gel state. ΔH and ΔS are respectively the change in enthalpy and change in entropy between the gel and fluid state. N_f is the number of lipids in the fluid state and N_{fg} is the number of interactions between gel and fluid state lipids. ω_{fg} is the interaction parameter between gel and fluid state lipids.

The two parameters, ΔH and ΔS, can be found by calorimetric measurements, leaving the interaction parameter ω_{fg} as a free parameter. The free parameter is estimated by the fitting of simulated heat capacity curves to the experimentally obtained.

In this project we aim to study the effect on permeability by a protein. For this we need to expand the model to contain pores (h) and a protein (p). Including these, leads to the following Gibbs free energy for a given state:

$$\begin{aligned} G = \quad & G_g + N_f \left(\Delta H - T\Delta S\right) \\ & + N_{fg}\omega_{fg} + N_{pf}\omega_{pf} + N_{pg}\omega_{pg} \\ & + N_{hg}\omega_{hg} + N_{pf}\omega_{hf} + N_{pg}\omega_{hg} \end{aligned} \tag{12}$$

Where N_{ij} is the number of interactions and ω_{ij} is the interaction parameter between i and j. Interactions between particles of same type are not regarded as interactions.

We use equations (8) and (12) to calculate the probability of accepting a change in state, in the performed Monte Carlo method.

The additional interaction parameters of the extended model have in this project been estimated from the literature (see section 5.1.1).

3.3 Considerations

In a Monte Carlo method a number of considerations have to be taken into account.

3.3.1 Equilibration

A random start configuration of the system is unlikely to be near the equilibrated state of the system. Equilibration of the system is therefore needed before sampling the data.

[6] A full description of equation (11) can be found in [14].

In general, it is difficult to determine the number of Monte Carlo cycles needed to equilibrate the system beforehand. The number of cycles depends on the interaction parameters and the number of interactions. Furthermore, the number of interactions depend on the size of the system and on the temperature. The range of temperatures of interest is fixed around the transition midpoint, leaving the size of the system as the only control parameter.

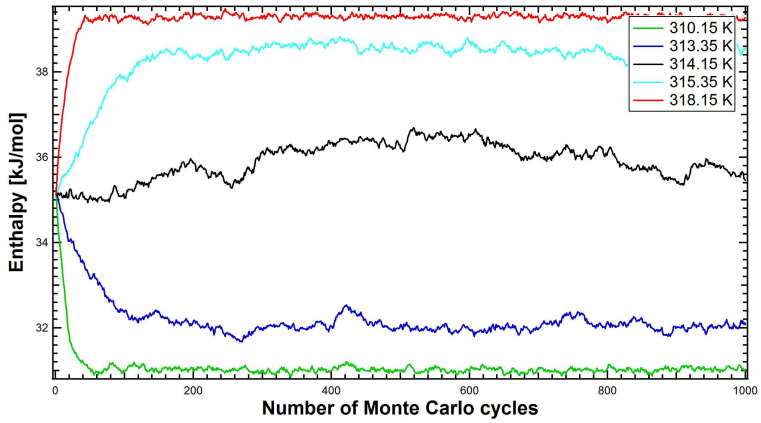

Figure 6: The approach to equilibrium starting from a random starting configuration. Equilibrium is reached when fluctuations settle around a stable enthalpy level. It can clearly be seen that at $T_m = 314.15$ K the fluctuations are larger and the cycles need to equilibrate are higher compared to away from transition.

From fig. 6 the number of Monte Carlo cycles needed to equilibrate at T_m, is of magnitudes higher than a 1000.

3.3.2 Finite system size

Any system possible to simulate, in reality, is of finite size. This introduces some errors when the correlation length[7] of the system is of the same order as the size of the system. To avoid these errors the system must be larger than the phenomena of interest. In the context of our project, the system has to be larger then the area of membrane affected by a protein.

3.4 Implementation of the Monte Carlo method

The method is carried out in small steps, such that any state of the system can be reached. Only one step is needed to describe a pure lipid membrane without pores. The melting or freezing of a lipid. For more complex systems a broader variety of steps is needed.

[7]The correlation length is the length scale of behaviors in the system.

The purpose of this project is to investigate how a protein can effect the permeability of the membrane. To describe this, three steps are needed: Creation of pores, closing of pores and diffusion (two particles switching positions). We have in our model chosen to have periodic boundaries (see [2] for details) to avoid boundary effects. This will also govern diffusion of the single protein, since the system can not distinguish between diffusion of lipids and diffusion of the protein.

The changing in lipid state as well as diffusion is directly handled in accordance with the Glauber algorithm (see section 3.1).

The dynamics for pore formation and closing, are based on observed area differences. A DPPC lipid changes its area by $\sim 25\%$ when changing from gel to fluid state [17]. From this a pore of the size of a gel state lipid can be created if its three nearest neighbors lipids are in the fluid state, and simultaneously change states, see equation (13) and figure 7.

$$A_{\text{before}} = 3 \cdot A_{\text{fluid}} = A_{\text{after}} = 3 \cdot A_{\text{gel}} + A_{\text{pore}} \tag{13}$$

A pore is closed in the opposite manner, i.e. if the three nearest neighbor lipids of the pore are in the gel state and change state simultaneously. To conserve energy and to keep the number of lipids constant in the system the lipid replaced by a pore is moved to the end of the lattice, hereby changing the size of the system by one. Equally, when a pore is closed a lipid is taken from the end of the lattice to fill the pore. These steps have been proposed in [4]. The creation and closing of pores is handled in accordance with the Glauber algorithm.

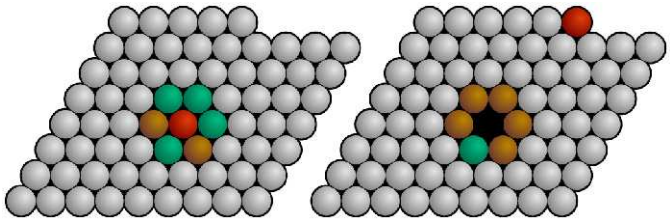

Figure 7: Illustration of the pore step (either formation or closing of pore). Green represents fluid state lipids while orange represents gel state lipids. The lipids are arranged in a triangular lattice. During the pore step three lipids change state simultaneously while the red particle (either a gel or fluid state lipid) is moved to or from the edge of the lattice. Illustration taken from [2]. The definition of nearest neighbor interactions, for the moved red particle, are described in [4]

3.4.1 Overview of Monte Carlo steps

The model used in this project has in essence been preformed in the following manner:

- Start setup:
  - Fill the system with lipids in gel and fluid state in a random manner.
  - Insert the protein into the system.

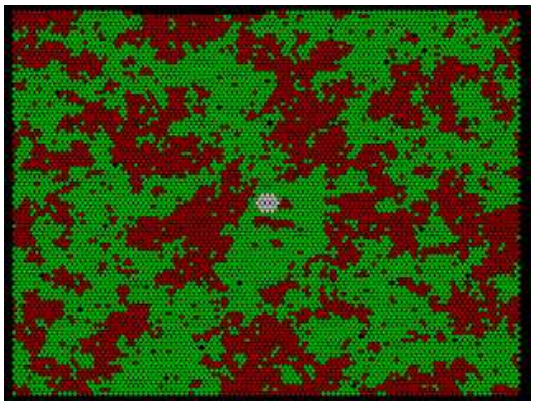

Figure 8: Snapshot of the system at phase transition. Gel phase lipids are red, fluid phase lipids are green, pores are black and the protein is white.

- Equilibration loop:
  - Try to melt gel into fluid or freeze fluid into gel.
  - Try to create pores and to close pores.
  - Let random particles diffuse (holes are also considered as particles). The protein is not diffusible.
- Monte Carlo loop:
  - The equilibration procedure is continued.
  - Data is sampled from the continued equilibration.

The used model described in detail in [2].

Part III
Experiments

This part will give a brief explanation of the experimental technique used to acquire some of the needed parameters[8] and the computer simulation itself. The techniques used are Differential Scanning Calorimetry (DSC) and the Monte Carlo method.

4 DSC

Differential scanning calorimetry is a technique that measures the amount of heat required to increase the temperature of a sample compared to that of a reference. The instrument (VP-DSC produced by Microcal (Northhampton/MA, USA)) consists of two, adiabatically separated cells: A reference and a sample cell. See appendix C for a illustration.

The instrument raises the temperature linearly with respect to time and measures the difference in heat flow between the two cells ($\Delta P = P_{\text{sample}} - P_{\text{reference}}$). The heat added to the system can be found by integrating over the excess power

$$\Delta Q = \int_t^{t+\Delta t} \Delta P(t')\mathrm{d}t' \simeq \Delta P \cdot \Delta t \tag{14}$$

where the approximation holds for small time intervals, which means a slow change in temperature. The difference in heat capacity, at constant pressure, between the two cells, is given by (see equation (2) for reference)

$$\Delta c_p = \left(\frac{\Delta Q}{\Delta T}\right)_p = \frac{\Delta P \cdot \Delta t}{\Delta T} = \frac{\Delta P}{\Delta T/\Delta t} \tag{15}$$

The expression $\Delta T/\Delta t$ is the scan rate of the calorimeter, which for all the experiments was 3 K/hour at constant pressure of 50 psi $\approx$ 3.4 atm.

Membrane melting temperature can directly be estimated by finding the main peak in the experimentally obtained heat capacity profile. Using equations (1) and (16) one can obtain the experimental values for ΔS and ΔH. The interaction parameter, ω_{fg}, has to be estimated through simulations and fitting of heat capacity curves (see [26] for more detail).

$$\Delta H = \int_{T_0}^{T_1} c_p \mathrm{d}T \tag{16}$$

[8] The change in enthalpy ΔH, the change in entropy ΔS, the melting point T_m, and the lipid interaction parameter ω_{fg}.

4.1 Sample preparation and extrusion

For the DSC experiments, large unilamellar vesicles of DPPC (Avanti Polar Lipids, Birmingham/AL, USA) were used. The sample was respectively prepared and extruded according to [27] and [28].

4.2 Data analysis

Four scans were preformed, and the best result is shown in fig. 9.

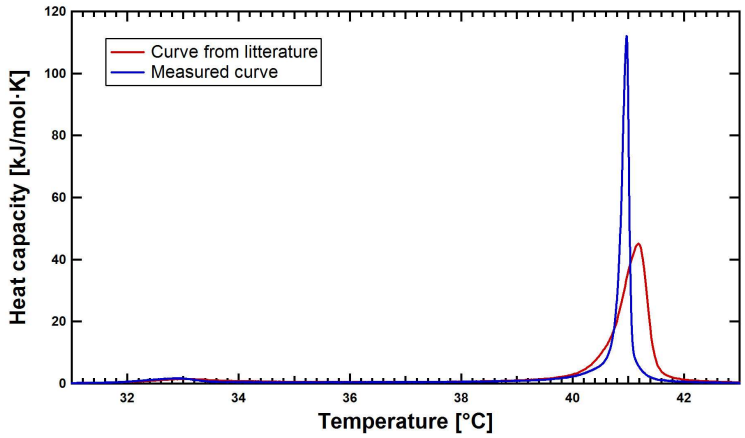

Figure 9: **Blue:** Measured excess heat capacity for DPPC measured by DSC. The first peak is pre-transition and the occurrence of it is discussed in [29]. The second peak is the main phase transition. **Red:** Reference heat capacity curve. Measured heat capacity curve for extruded large unilamellar vesicles of DPPC by DSC with at scan rate of 5 K per hour. This data has been provided by Thomas Heimburg, Niels Bohr Institute, University of Copenhagen.

The raw data was normalized by concentration and baseline corrected. The parameters obtained from the experiment are shown in table 1.

ΔH	32170.0 J/mol
ΔS	102.0 J/mol· K
T_m	40.97°C

Table 1: Experimental data from DSC, for extruded large unilamellar DPPC vesicles.

4.2.1 Discussion of experimental results

Thermodynamic properties such as ΔH, ΔS and T_m depend on baseline correction. A small variation in the baseline can result in a huge variation of the parameters. A complete investigation of error due to baseline correction, is a project in itself, and was therefore not done.

By comparing the measured heat capacity to a reference curve (see fig. 9), two discrepancies are apparent, the width and height of the heat capacity curve. This indicates an error in the results obtained from DSC. If one further compares the obtained results with other work for multilamellar vesicles [26], it suggests that our sample contained a combination of multilamellar and unilamellar vesicles. This is an indication that our extrusion process wasn't quite successful.

4.2.2 Determination of interaction parameter

The interaction parameter ω_{fg} is obtained by fitting the simulated heat capacity curves[9] for various values of interaction parameters, over the experimental curve and looking for the best match[10] (for more detail see [26]). All the simulated heat capacity curves are based on the experimentally found values from table 1. The obtained value for the interaction parameter is $\omega_{fg} = 1385.9 J/mol$.

The found value for the interaction parameter is close to the critical slowdown value[11] of $\omega = 1434.77$ J/mol [30]. Because of this, the amount of Monte Carlo cycles needed to equilibrate the system and to get decent statistics will increase [2]. To finish the project within the given time frame we have chosen to use data from [2] (see table 2).

[9] In these simulations there was no protein and pore formation was prohibited.

[10] A better, but more time consuming, way is described in [23].

[11] Critical slowdown dictates the number of Monte Carlo cycles needed to equilibrate the system. At the critical value one would need an infinite number of cycles to equilibrate the system [2]. The critical value is $\omega_c = RT_m \frac{\ln 3}{2} = 1434.77$ J/mol for $T_m = 314.15$ K.

5 Simulation

This section will give a brief overview of the simulation setup and the parameters used. The rest of the section is devoted to simulation results.

5.1 Simulation setup

All simulations were performed on a $100 \times 100 + 50$ lattice. The 50 is an incomplete row in the lattice, into which lipids are placed when a pore is created in the system. This is done to avoid creation and deletion of rows, which will slow down the program.

The simulations are allowed to equilibrate for $N_{eq} \simeq 2 \times 10^4$ Monte Carlo cycles where only changes in the state of the lipids and diffusion[12] is allowed.

The program further allows the system to equilibrate for an equal amount of Monte Carlo cycles where also pore creation and closing is allowed. By dividing the equilibration in two, the Monte Carlo cycles needed are minimized.

The data sampling is done over 10^5 Monte Carlo cycles, where all simulation steps are allowed (diffusion, lipid melting and freezing and pore formation and closing).

We have chosen to model the single protein in this project as an round-shaped object of the size of seven lipids[13], which we have fixed in the center of the lattice. Fixing the position of the protein in the simulations enables direct study of the protein effect on the neighboring membrane.

The parameters used in the simulation can be seen in table 2.

ΔH	36400 J/mol
ΔS	115.9 J/mol· K
T_m	41.0°C
ω_{fg}	1326.0 J/mol
ω_{fh}	2254.2 J/mol
ω_{gh}	4508.4 J/mol
ω_{ph}	13260.0 J/mol

Table 2: Parameters used in the simulation of DPPC.

[12] It can be argued that diffusion is not relevant for at system containing only a stationary protein and lipids. It is however incorporated into this part of the simulation to ensure generality.

[13] This has been chosen in accordance with previous studies of proteins [26].

5.1.1 Consideration of chosen parameters

In the literature [26] simulations studies have been conducted of membranes containing the polypeptide, Gramicidin A. A polypeptide is not generally the same as a protein, but in the context of this project there is no actual difference. The interaction parameters for Gramicidin A with fluid and gel state lipids were estimated to be of the same magnitude as the fluid-gel interaction parameter. It is on this basis we estimated our protein interaction parameters.

Experiments have shown that a DPPC bilayer has around 50 pores per mm^2 in the phase transition [31]. The size of the simulated system is approximately an eighth of this area. To avoid unsatisfying statistics on pores we have chosen to lower the pore interaction parameters, hereby increasing the probability of pores.

We have further chosen to set pore-pore interactions extremely high to avoid pore aggregations, since this has a tendency to make the simulation crash [2]. This can be justified to some degree by the low number of pores in a real membrane.

Furthermore, pore-protein aggregation is not allowed, to avoid scenarios where the protein is not completely embedded in the membrane.

5.2 Simulation results

In the following section, the simulation results will be presented and analyzed.

To investigate the effect of a protein on a lipid membrane, all pores have been stored with their relative distance from the edge of the protein. This is done for each Monte Carlo cycle. The distance is calculated in units of lipid diameter. The state fluctuations (probability for a lipid changing state) have been sampled in a similar fashion. Under fluctuation sampling creation, closing and diffusion of pores where not allowed. This can result in minor alterations of the protein induced effect, but the general behavior should be maintained.

5.2.1 Investigation of protein behavior

To investigate the nature of the protein effect, three different types of proteins have been considered. The types of protein have been chosen such that they can illustrate categoric behavior of proteins[14]. The three types of protein are the following:

- A fluid state loving protein, $\omega_{pf} = 0$ and $\omega_{pg} = \omega_{fg} = 1326.0$ J/mol
- A gel state loving protein, $\omega_{pg} = 0$ and $\omega_{pf} = \omega_{fg} = 1326.0$ J/mol
- A protein that likes fluid and gel state equally, $\omega_{pg} = \omega_{pf} = 0.0$ J/mol

Due to the small size of the protein the overall physics of the system is conserved independent of protein type. Therefore the effect of the different proteins can be directly compared. The heat capacity of the system with the three proteins and the protein free system are compared in appendix D.

The effect on permeability and state fluctuations induced by a fluid state loving protein can be seen in fig. 10-11 and for a gel state loving protein in fig. 12-13.

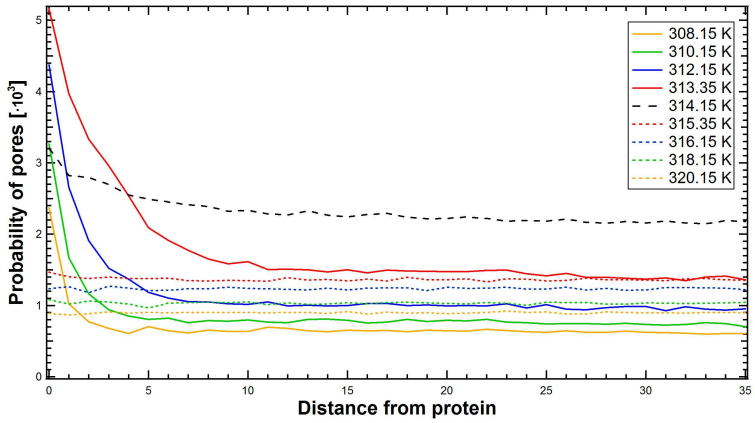

Figure 10: Probability of finding a pore at a given distance from a fluid state loving protein. Different colors represent different temperatures relative to transition. Full lines represent temperatures lower than the transition temperature. Dotted lines represent temperatures higher than or equal to the transition temperature.

As seen in fig. 10-11 the fluid state loving protein induces higher permeability and higher state fluctuations in the neighboring area, at temperatures below phase the transition. This effect gets more pronounced close to the phase transition temperature. Above the phase transition there is no pronounced effect to be seen.

[14]Real proteins can be expected to display more complicated interaction behavior [26], but this is outside the scope of this project.

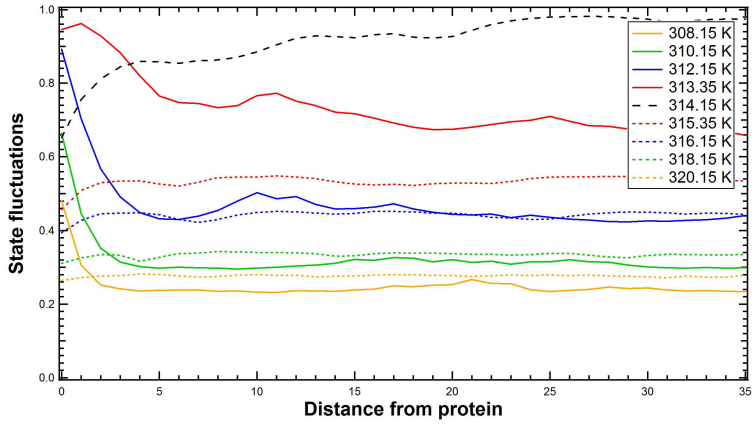

Figure 11: State fluctuations as a function of distance from a fluid state loving protein. Different colors represent different temperatures relative to transition. Full lines represent temperatures lower than the transition temperature. Dotted lines represent temperatures higher than or equal to the transition temperature. The irregular bumps in the state fluctuations can be attributed to pores in the system which also induce fluctuations.

For temperatures below and above phase transition the behavior of the permeability is similar to that of the state fluctuations. Only at the transition temperature there is a clear difference in the behavior of the permeability and the state fluctuations.

The fashion, in which the state fluctuations are sampled, can not be expected to contain all information about actual fluctuations of the system, since pore creation, closing and diffusion is prohibited. This becomes apparent at phase transition temperatures since the state fluctuations are maximal. We will because of this not consider state fluctuations at the phase transition temperature.

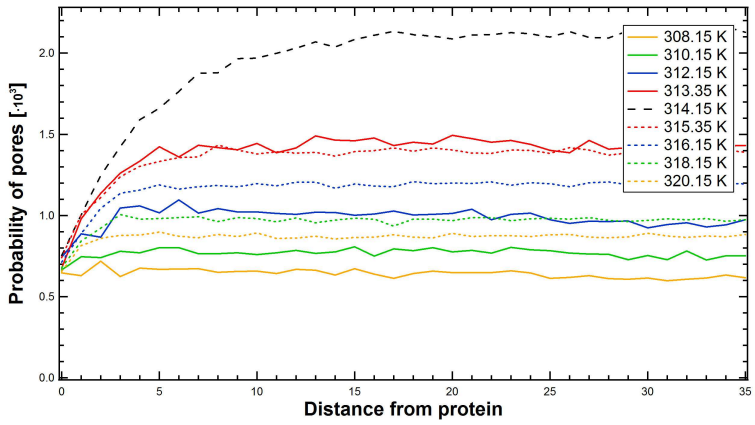

Figure 12: Probability of finding a pore at a given distance from a gel state loving protein.

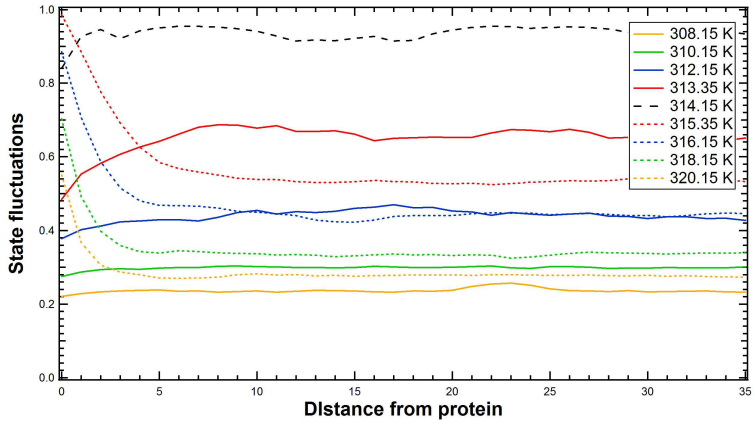

Figure 13: State fluctuations as a function of distance from a gel state loving protein.

Fig. 12 shows that the gel state loving protein induces a lowering of the permeability in the local neighborhood at all temperatures. This effect of the protein gets more pronounced when approaching phase transition temperature.

This behavior is not shared by the state fluctuations, fig. 13, which show a increase near the protein for temperatures above phase transition. This behavior can be explained by the used permeability model, which promotes pores in a fluid environment, which will lead to diffusion of pores from the protein induced gel environment to fluid environments away from the protein.

The protein that likes gel state and fluid state equally, represents a third category of protein. This protein type only induces minor changes in the neighboring membrane. Its behavior is shown in appendix E.

The investigation of different types of protein indicates that proteins can induce large changes in the neighboring lipid membrane and that these changes vary fundamentally depending on lipid-protein interactions. We have with this simple protein model observed both promoting and inhibiting effects regarding permeability. The results further indicate that the protein influences an area of about 500 lipids close to the phase transition. This indicates that the protein effects can influence macroscopic behavior of membranes.

5.2.2 Investigation of protein effect dependence on membrane interactions

It has been shown that a number of external parameters have comprehensive impact on the behavior of cell functions. External parameters such as anaesthetics change the physical properties of the membrane [8]. Changes of this nature are shown in the form of a shift in transition temperature and a change of the width and height of the heat capacity curve. To investigate the impact of these type of changes on the protein effect on the lipid membrane, simulations with different interaction parameters, ω_{fg}, have been conducted with a fluid state loving protein. By changing the interaction parameter between gel and fluid state lipids, the width and height of the heat capacity curve will change, while the area under the curve will stay constant [2]. The unique phenomena displayed at phase transition are correlated to the height and sharpness of the heat capacity curve. A sharp heat capacity curve will sharpen the transition, making transition effects more pronounced, while a broadening of the heat capacity will result in a broader transition which disperse the transition effects.

The behavior of the heat capacity curve influences a broad spectra of physical properties[15] of the membrane, among these the permeability [2]. This correlation is illustrated in fig. 14 with three different ω_{fg} values[16].

[15]The behavior of the heat capacity curve will also influence the average domain size and hereby the correlation length of the system.

[16]The three ω_{fg} values investigated; ω_{fg} = 1376.0 J/mol, 1326.0 J/mol and 1276.0J/mol.

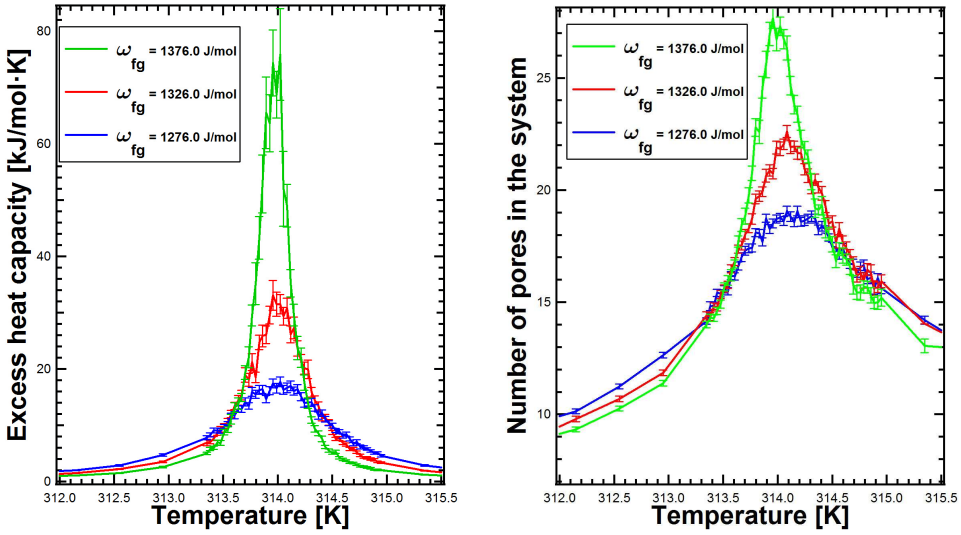

Figure 14: **Left:** Comparison of simulated heat capacitys for the different ω_{fg} values. **Right:** Comparison of average number of pores in the entire system for different values of the interaction parameter.

Fig. 14 further shows that for temperatures away from the transition the lowest interaction parameter has the highest heat capacity and permeability. As nearing transition the high interaction parameter leads to the highest heat capacity and permeability. From the figures, it can be seen that this shift occurs at a critical point, $T \sim 313.5$ K. This behavior can also be seen away from the protein in fig. 15.

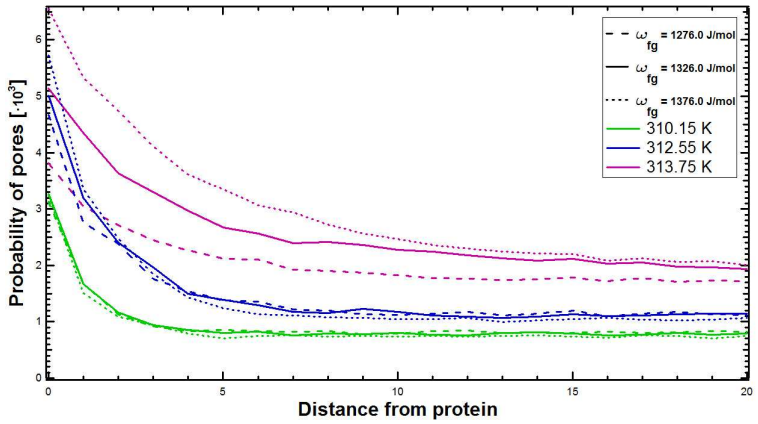

Figure 15: Probability of pores at a given distance from a fluid state loving protein, normalized with the probability of pores in a pure lipid membrane (without protein).

However fig. 15 shows for $T = 312.55$ K that the protein induces the shift in the neighboring membrane. The shift induced by a protein indicates that this type of protein changes the local membrane state towards phase transition.

The investigation of different values for the interaction parameters indicate that protein effect on the nearby membrane is highly sensitive to variation.

5.2.3 Comparison of results with literature

Simulation studies have been conducted, investigating the hydrophobic matching effect on membrane thickness around a fluid loving protein [10]. It was found that this behavior followed equation (17)[17].

$$\frac{\langle d_L(I)\rangle_T}{\langle d_L^0\rangle} = 1 + \left(\frac{d_p}{\langle d_L^0\rangle} - 1\right) e^{-D(I)/\xi_p(T)} \tag{17}$$

Where $\langle d_L(I)\rangle_T$ is the average thickness of the membrane at a given distance step I. $\langle d_L^0\rangle$ is the average membrane thickness away from the protein and d_p is the thickness of the protein. D is the diameter of a lipid and ξ_p is the decay length.

Changes in membrane thickness are related to compressibility which is correlated to permeability [8]. The permeability of the membrane around the protein can therefore be expected to display a behavior similar to that of equation (17). To investigate this similarity, a selection of sampled data has been divided by non-protein containing simulation data and fitted to equation (18).

$$F(r)_T = 1 + B \cdot \exp\left(\frac{-r}{A(T)}\right) \tag{18}$$

A describes the decay length of the protein behavior. B indicates the magnitude of the behavior. C is the offset.

[17] The presented equation has been divided by $\langle d_L^0\rangle$. The is done so comparison with our data can be done directly.

$Temperature(K)$	A	B	C
308.15	0.58 ± 0.03	2.56 ± 0.04	1.004 ± 0.005
310.15	1.07 ± 0.04	2.77 ± 0.04	0.997 ± 0.006
312.15	1.91 ± 0.05	2.57 ± 0.04	1.001 ± 0.006
313.35	3.04 ± 0.09	2.55 ± 0.04	1.014 ± 0.008

Table 3: Fit parameters for a fluid loving protein in a $\omega_{fg} = 1326.0$ J/mol membrane.

The found fit parameters are seen in table 3 and the actual fit on fig. 16.

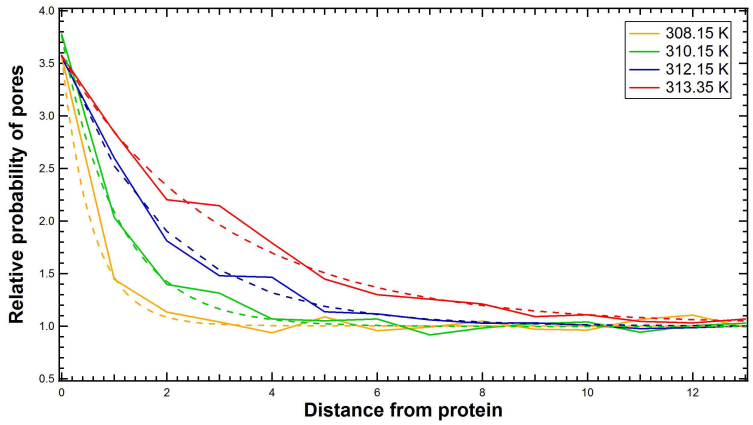

Figure 16: Relative probability of pores for a fluid loving protein in a $\omega_{fg} = 1326.0$ J/mol membrane. The dotted lines represents the fitted equation (18).

From table 3 and fig. 16 it seem that our results agree with that of the literature. From the fit values it can be seen that the decay length of the protein increases when approaching transition, whereas the magnitude of the decay decreases. Fig. 16 indicates that, independent of temperature, the permeability at the protein edge is a factor 4 larger than normal permeability at each given temperature.

Part IV
Conclusion and perspectives

6 Conclusion

Assuming that the numerical simulations contained the essential physics of a membrane, our simple model indicates that different types of protein can induce large changes in the neighboring lipid membrane. The nature of these changes vary fundamentally depending on the lipid-protein interactions. Both permeability promoting and inhibiting changes of neighboring lipids have been observed.

The results indicate that the changes induced by a protein can influence a large number of lipids, making it possible to influence the macroscopic behavior of a membrane. Our simple model further indicates that the influence of a protein is highly sensitive to variation of the overall physics of the membrane. Our results are in good agreement with a known model [10].

To answer the question raised in the introduction:

It is possible that channel events typically attributed to proteins originate from lipids.

7 Perspectives

The possibility of protein induced lipid channel events, has far reaching consequences for the understanding of lipid membranes. To fully explore this possibility further research is necessary.

The first step, would be to enhance the simple model used in this project, such that it takes more complex lipid-protein interactions into account. Obvious alterations could be to let the protein change conformation state due to interactions with the membrane or due to external parameters.

The second step, would be to incorporate collective protein behavior. Studies of protein aggregation and how these aggregates influence the permeability of the membrane.

The final step would be to design experiments that can validate these predictions.

A better understanding of membranes could result in the designing of function specific proteins, which will enable control of membrane functions. Far reaching applications could be a new generation of drugs and drug delivery systems.

Part V
Appendix

A Transition temperature

The lipid melting transition occurs, for DPPC, in a temperature interval smaller than 1 K. In this small temperature region a large amount of enthalpy is absorbed by the membrane. Such transition can be described by the membrane temperature transition, T_m, and melting enthalpy. The entropy change in a sharp transition can be described by:

$$\Delta S = \int_{T_m-\delta}^{T_m+\delta} \frac{c_p}{T} \mathrm{d}T \approx \frac{1}{T_m} \int_{T_m-\delta}^{T_m+\delta} c_p \mathrm{d}T = \frac{\Delta H}{T_m} \tag{19}$$

Where δ is a small temperature interval.

B Fluctuations

Derivation of equation (5) using the fluctuation dissipation theorem.

$$\begin{aligned}
c_p &= \left(\frac{\mathrm{d}\langle H\rangle}{\mathrm{d}T}\right)_p, \qquad \langle H\rangle = \frac{\sum_i H_i \cdot e^{-H_i/RT}}{\sum_i e^{-H_i/RT}} && (20)\\
&= \left(\frac{\mathrm{d}}{\mathrm{d}T}\frac{\sum_i H_i \cdot e^{-H_i/RT}}{Z}\right)_p, \qquad Z = \sum_i e^{-H_i/RT} && (21)\\
&= \frac{\sum_i H_i^2 \cdot e^{-H_i/RT}}{RT^2 \cdot Z} - \frac{1}{RT^2}\frac{\sum_i H_i \cdot e^{-H_i/RT}}{Z}\frac{\sum_j H_j \cdot e^{-H_j/RT}}{Z} && (22)\\
&= \frac{\langle H^2\rangle - \langle H\rangle^2}{RT^2} && (23)
\end{aligned}$$

Where the indices i, j denote the different states the system can be in, R is the gas constant and T is the temperature. The sum is over all possible states.

Derivation of equation (7)

$$\begin{aligned}
\kappa_T^A &= -\left(\frac{1}{\langle A\rangle}\cdot\frac{\mathrm{d}\langle A\rangle}{\mathrm{d}\Pi}\right)_T, \qquad \langle A\rangle = \frac{\sum_i A_i \cdot e^{-H_i/RT}}{\sum_i e^{-H_i/RT}} && (24)\\
&= -\frac{1}{\langle A\rangle}\left(\frac{\mathrm{d}}{\mathrm{d}\Pi}\frac{\sum_i A_i \cdot e^{-H_i/RT}}{Z}\right)_T && (25)\\
&= \frac{\langle A^2\rangle - \langle A\rangle^2}{\langle A\rangle RT} && (26)
\end{aligned}$$

Where Π is the lateral pressure and the enthalpy is $H = U + pV + \Pi A$.

C Differential scanning calorimeter

The sample and reference cell are enclosed by a adiabatic shield, to prevent heat leakage. The temperature difference between the two cells is kept zero, while the calorimeter raises the temperature linearly. The difference between heat flows to the cells, ΔP, is measured and is proportional to the excess heat capacity (see equation (15)).

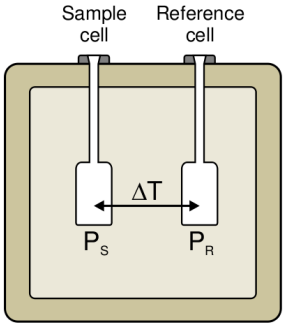

Figure 17: Schematic drawing of how DSC works. The temperature difference between the two samples is kept equal while the temperature is raised linearly. Illustration taken from [2].

D Comparison of heat capacity curves

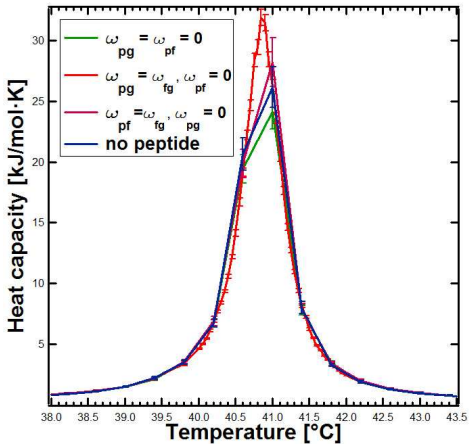

Figure 18: Comparison of simulated heat capacity curves for a system containing different types of proteins. A pure membrane, with no protein, has been plotted for reference. Due to fewer data points, there are some discontinuities in three heat capacity curves.

As can be seen in fig. 18 the heat capacity curves are almost identical for

different types of proteins, the small discrepancies are due statistical errors.

E Third type of protein

Fig. 19, which shows an increased permeability near the protein for temperatures below phase transition. This effect gets slightly more pronounced when approaching the transition temperature. As expected there is no apparent effect of the protein at the transition. Above phase transition no pronounced effect on permeability can be seen. Fig. 20 shows a slight increase in the state fluctuations around the protein, at temperatures both below and above the transition. At transition no pronounced effect of the protein is seen. For temperatures at transition and below, the protein effect on permeability follows that of the state fluctuations. for temperatures above transition effects similar to those seen for the gel loving protein is displayed.

The simulation indicates that proteins of this category have no pronounced effect on the nearby membrane.

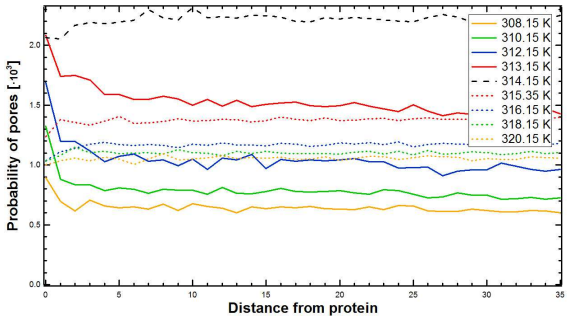

Figure 19: Probability of pores as a function of distance form a protein.

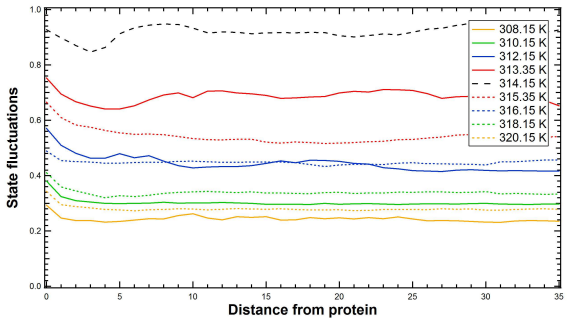

Figure 20: State fluctuations as a function of distance form a protein.

References

[1] S. Singer and G. L. Nicolson, Science **175**, 720 (1972).

[2] A. Blicher, Permeability studies of lipid vesicles by fluorescence correlation spectroscopy and monte carlo simulations, Master's thesis, Niels Bohr Institute; University of Copenhagen, 2007.

[3] H. Khandelia, J. H. Ipsen, and O. G. Mouritsen, Biochim. Biophys. Acta **1778**, 1528 (2008).

[4] K. Wodzinska, A. Blicher, and T. Heimburg, The thermodynamics of lipid ion channel formation in the abstence and presence of anesthetics. blm experiments and simulations, arXiv:0902.2271v2 [Physycs.bio-ph].

[5] D. Papahadjopoulos, K. Jacobson, S. Nir, and T. Isac, Biochim. Biophys. Acta **311**, 330 (1973).

[6] J. F. Nagle and H. L. Scott, Biochim. Biophys. Acta **513**, 236 (1978).

[7] V. F. Antonov, V. V. Petrov, A. A. Molnar, D. A. Predvoditelev, and A. S. Ivanov, Nature **283**, 585 (1980).

[8] A. Blicher, K. Wodzinska, M. Fidorra, M. Winterhalter, and T. Heimburg, The temperature dependence of lipid membrane permeability, its quantized nature, and the influence of anesthetics, arXiv:0807.4825v1 [Physycs.bio-ph].

[9] K. Kaufmann and I. Silman, Biophysical Chemistry **18**, 89 (1983).

[10] M. M. Sperotto and O. G. Mouritsen, Biophysical Journal **59**, 261 (1991).

[11] J. A. Killian and T. Nyholm, Current Opinion in Structural Biology **16**, 473 (2006).

[12] E. Ising, Z. Phys. **31**, 253 (1925).

[13] M. J. Janiak, D. M. Small, and G. G. Shipley, The Journal of Biological Chemistry **254**, 6068 (1979).

[14] T. Heimburg, *Thermal Biophysics of Membranes*, 1st ed. (Wiley-VCH, 2007).

[15] M. L. gudmundsson, Phase behavior in lipid tethers and vesicles - a thermodynamic study, Master's thesis, Niels Bohr Institute; University of Copenhagen, 2007.

[16] T. L. Hill, *An Introduction to Statictical Thermodynamics*, 1st ed. (Dover Publications Inc., 1986).

[17] T. Heimburg, Biochim. Biophys. Acta **1415**, 147 (1998).

[18] F. Dumas, M. C. Lebrun, and J. Tocanne, FEBS Letters **458**, 271 (1999).

[19] F. Dumas, M. M. Sperotto, M. Lebrun, J. Tocanne, and O. G. Mouritsen, Biophysical Journal **73**, 1940 (1997).

[20] R. J. Glauber, The Journal of Mathematical Physics **4**, 294 (1963).

[21] D. A. Pink, T. J. Green, and D. Chapman, Biochemistry **19**, 349 (1990).

[22] O. G. Mouritsen *et al.*, J. Chem. Phys. **79**, 2027 (1983).

[23] V. P. Ivanova and T. Heimburg, Phys. Rev. E, **63**, 1914 (2001).

[24] S. Doniach, The Journal of Chemical Physics **68**, 4912 (1978).

[25] I. P. Sugár, R. L. Biltonen, and N. Mitchard, Methods in Enzymology **240**, 569 (1994).

[26] V. P. Ivanova, I. M. Makarov, T. E. Schäffer, and T. Heimburg, Biophysical Journal **84**, 2427 (2003).

[27] J. B. R. N. Berger, A. Sachse and M. Brandl, International Journal of Pharmaceutics **223**, 55 (2001).

[28] B. P. M. K. T. N. K. S. R. C. MacDonald, R. I. MacDonald and L. Hu, Biochim. Biophys. Acta **1061**, 297 (1991).

[29] T. Heimburg, Biophysical Journal **78**, 1154 (2000).

[30] G. H. Wannier, Reviews of Modern Physics **17**, 50 (1945).

[31] V. F. Antonov, A. A. Anosov, V. P. Norik, and E. Y. Smirnova, European Biophysical Journal **34**, 155 (2005).